16. The protein is predicted to be largely helical [B. Rost and C. Sander, *Proteins* **19**, 55 (1994)], but prediction-based threading [B. Rost, in *Protein Folds, A Distance-Based Approach*, H. Bohr and S. Brunak, Eds. (CRC Press, Boca Raton, FL, 1995), pp. 132–151; B. Rost, in *The Third International Conference on Intelligent Systems for Molecular Biology (ISMB)*, C. Rawlings *et al.*, Eds. (AAAI Press, Menlo Park, CA, 1995), pp. 314–321] fails to identify any other proteins of similar structure; http://www.embl-heidelberg.de/predictprotein/predictprotein.html.
17. T. E. Creighton, *Proteins: Structures and Molecular Properties* (Freeman, New York, ed. 2, 1993).
18. A. Schöler and H. J. Schüller, *Mol. Cell. Biol.* **14**, 3613 (1994); M. Proft, D. Grzesitza, K. D. Entian, *Mol. Gen. Genet.* **246**, 367 (1995).
19. All yeast manipulations were in the SEY6210 background (*MAT***a**, *leu2-3, ura3-52, his3-Δ200, lys2-801, trp1-Δ901, suc2-Δ9*). The *CAT5/COQ7* locus was disrupted with a PCR-mediated approach [A. Baudin, O. Ozier-Kalogeropoulos, A. Denouel, F. Lacroute, C. Cullin, *Nucleic Acids Res.* **21**, 3329 (1993); the primers used were SHP84 and SHP85]. The *CAT5/COQ7* gene was entirely replaced with a DNA fragment containing a disruption module encoding the green fluorescent protein and the *HIS3* gene [R. K. Niedenthal, L. Riles, M. Johnston, J. H. Hehemann, *Yeast* **12**, 773 (1996)]. Haploid cells were transformed [R. D. Gietz, R. H. Schiestl, A. R. Willems, R. A. Woods, *ibid.* **11**, 355 (1995)] with the PCR product, and *HIS3* integrants were selected on minimal medium lacking histidine. Gene disruptions were confirmed by PCR analysis with primers SHP82, SHP83, and ML138. The Δ*cat5/coq7* strain failed to grow (*24*) on YEPG or $YEPE_3$, which contains ethanol (*11*). The sequences of the primers are available on request.
20. The *CAT5/COQ7* locus was directly amplified from yeast genomic DNA by PCR with *Pfu* polymerase (Stratagene) and primers SHP69 and SHP70. A cDNA corresponding to the entire *clk-1* coding sequence was obtained by PCR amplification, also with *Pfu* polymerase, and nested primer pairs SHP57 and SHP59 and then SHP57 and SHP58 on single-stranded cDNA that had been synthesized by priming with SHP59. The respective yeast and nematode PCR products were digested with Hind III and ligated to Hind III–cut and dephosphorylated pVT102-U [T. Vernet, D. Dignard, D. Y. Thomas, *Gene* **52**, 225 (1987)]. As well as restoring growth on glycerol, both the *CAT5/COQ7*- and *clk-1*–containing plasmids restored the ability of the Δ*cat5/coq7* strain to grow on ethanol [$YEPE_3$ medium (*24*)]. The Δ*cat5/coq7* strain transformed with the *CAT5/COQ7*-containing plasmid did not grow as well as the wild-type yeast strain on nonfermentable carbon sources. When the yeast gene was reintroduced in the context of its own promoter on a centromeric vector, full restoration of wild-type growth was obtained (*24*). *CAT5/COQ7* is known to be involved in the regulation of its own expression (*11*); presumably, the presence of excess Cat5p/Coq7p perturbs the normal metabolic balance of yeast. The sequences of the primers are available on request.
21. E. W. Jones, J. R. Pringle, J. R. Broach, Eds., *The Molecular and Cellular Biology of the Yeast* Saccharomyces (Cold Spring Harbor Laboratory Press, Cold Spring Harbor, NY, 1992).
22. J. Campisi, *Cell* **84**, 497 (1996); L. Guarente, *ibid.* **86**, 9 (1996).
23. T. M. Barnes, Y. Jin, H. R. Horvitz, G. Ruvkun, S. Hekimi, *J. Neurochem.* **67**, 46 (1996).
24. B. Lakowski and J. Ewbank, unpublished data.
25. By picking Sma non-Dpy recombinant progeny of *dpy-17(e164) sma-4(e729)/unc-79(e1030) clk-1(e2519) lon-1(e185)* hermaphrodites, we were able to position *clk-1* more precisely: *dpy-17* 25/79 *clk-1* 27/79 *lon-1* 27/79 *sma-4*. To interpolate the physical position of *clk-1*, we estimated that the separation between *ced-4* and *dpy-17* is ~0.2 centimorgans on the basis of data in the database ACeDB (*7*). By using linked double mutants, we also directly determined (*24*) the two point distances between *dpy-17* and *sma-4* (0.85 cM), *dpy-17* and *lon-1* (0.5 cM), and *lon-1* and *sma-4* (0.35 cM). Details of the mapping data can be found in ACeDB (*7*).
26. The sequencing of allele *qm11*, which has a phenotype essentially identical to *e2519* (*1*), revealed an identical lesion. The low probability of independently obtaining the same mutation twice suggests that the original allele was lost. Sequencing of *qm47* failed to reveal a mutation. Subsequent reexamination of the phenotype of *qm47* homozygotes and new complementation tests suggest that *qm47* is not a *clk-1* allele.
27. We thank A. Coulson for cosmids; K. Kemphues for strains; J.-C. Labbé, A Kothari, and J. Mes-Mason for nematode, mouse, and human RNA, respectively; and A. Wong, A.-M. Sdicu, and R. Durbin. Some nematode strains used in this work were provided by the Caenorhabditis Genetics Center, which is funded by the NIH National Center for Research Resources. Supported by a Royal Society–National Science and Engineering Research Council of Canada exchange fellowship and a Medical Research Council of Canada fellowship to J.J.E., a Medical Research Council of Canada grant to S.H., a Canadian Genome Analysis and Technology grant to H.B., and by fellowships to B.L. from the J. W. McConnell Foundation and Fonds pour la Formation de Chercheurs et l'Aide à la Recherche Québec.

3 September 1996; accepted 18 December 1996

Structure of Bcl-x_L–Bak Peptide Complex: Recognition Between Regulators of Apoptosis

Michael Sattler, Heng Liang, David Nettesheim, Robert P. Meadows, John E. Harlan, Matthias Eberstadt, Ho Sup Yoon, Suzanne B. Shuker, Brian S. Chang, Andy J. Minn, Craig B. Thompson, Stephen W. Fesik*

Heterodimerization between members of the Bcl-2 family of proteins is a key event in the regulation of programmed cell death. The molecular basis for heterodimer formation was investigated by determination of the solution structure of a complex between the survival protein Bcl-x_L and the death-promoting region of the Bcl-2–related protein Bak. The structure and binding affinities of mutant Bak peptides indicate that the Bak peptide adopts an amphipathic α helix that interacts with Bcl-x_L through hydrophobic and electrostatic interactions. Mutations in full-length Bak that disrupt either type of interaction inhibit the ability of Bak to heterodimerize with Bcl-x_L.

Programmed cell death (apoptosis) occurs during the course of several physiological processes, and when dysregulated contributes to many diseases, including cancer, autoimmunity, and neurodegenerative disorders (*1*). The Bcl-2 family of proteins plays a central role in the regulation of apoptotic cell death induced by a wide variety of stimuli (*2*). Some proteins within this family, including Bcl-2 and Bcl-x_L, inhibit programmed cell death, and others, such as Bax and Bak, can promote apoptosis. Interactions between these two groups of proteins antagonize their different functions and modulate the sensitivity of a cell to apoptosis (*3*, *4*). Several regions of the death-inhibiting proteins participate in their antiapoptotic activity and heterodimerization with the death-promoting proteins, including the Bcl-2 homology 1 (BH1) and BH2 regions (*3*, *5*, *6*). In contrast, only a relatively small portion of the death-promoting proteins encompassing the BH3 region is critical for the ability to promote apoptosis (*7*– *10*). For example, small, truncated forms of Bak are necessary and sufficient both for promoting cell death and binding to Bcl-x_L (*7*).

The three-dimensional (3D) structure of the cell survival protein Bcl-x_L consists of two central hydrophobic α helices surrounded by five amphipathic helices (*11*). To understand how Bak interacts with Bcl-x_L and inhibits the ability of Bcl-x_L to promote cell survival, we determined the solution structure of Bcl-x_L complexed with a 16-residue peptide derived from the BH3 region of Bak. We also measured the binding affinities of Bcl-x_L to alanine mutant Bak peptides and to peptides corresponding to the BH3 regions of other Bcl-2 family members (*12*, *13*).

The minimal region of Bak required to bind to Bcl-x_L was examined in a fluorescence-based assay (*14*). A 16–amino acid peptide derived from the BH3 region of Bak (residues 72 to 87) bound tightly to Bcl-x_L (Table 1). In contrast, smaller peptides from this region, such as an 11–amino acid peptide corresponding to residues 77 to 87, did not bind (Table 1). The 16–amino acid peptide of Bak corresponds precisely to the

M. Sattler, H. Liang, D. Nettesheim, R. P. Meadows, J. E. Harlan, M. Eberstadt, H. S. Yoon, S. B. Shuker, S. W. Fesik, Pharmaceutical Discovery Division, Abbott Laboratories, Abbott Park, IL 60064, USA.
B. S. Chang, A. J. Minn, C. B. Thompson, Howard Hughes Medical Institute and Departments of Medicine, Molecular Genetics, and Cell Biology, University of Chicago, Chicago, IL 60637, USA.
*To whom correspondence should be addressed.

region of Bcl-x_L that forms the second α helix (*11*).

The structure of the 16–amino acid peptide (*15*) complexed with a biologically active deletion mutant of Bcl-x_L (*16*) was determined by nuclear magnetic resonance spectroscopy (NMR). The structure was determined from a total of 2813 NMR-derived restraints and is well defined by the NMR data (Fig. 1A) (*17*). The atomic root-mean-square deviation (rmsd) about the mean coordinate positions for residues 1 to 205 of Bcl-x_L and 72 to 87 of the Bak peptide was 0.79 ± 0.15 Å for the backbone and 1.21 ± 0.13 Å for all heavy atoms.

Overall, the structure of the truncated form of Bcl-x_L when complexed to the Bak peptide is similar to the x-ray and NMR structures of uncomplexed Bcl-x_L (*11*, *18*). The Bak peptide binds in a hydrophobic cleft formed by the BH1, BH2, and BH3 regions of Bcl-x_L (Figs. 1 and 2). Although a random coil when free in solution (*19*), the Bak peptide forms an α helix when complexed to Bcl-x_L. The NH_2-terminal residues of the peptide show numerous nuclear Overhauser effects (NOEs) to residues in the BH1 region of Bcl-x_L (Val^{126}, Glu^{129}, Leu^{130}, and Phe^{146}), whereas the COOH-terminal portion of the Bak peptide interacts predominantly with residues in the BH2 and BH3 regions (Phe^{97}, Arg^{100}, Tyr^{101}, and Phe^{105}). The hydrophobic side chains of the peptide (Val^{74}, Leu^{78}, Ile^{81}, and Ile^{85}) point into a hydrophobic cleft of Bcl-x_L (Fig. 2) and stabilize complex formation. In addition to these hydrophobic interactions, the charged side chains of the Bak peptide (Arg^{76}, Asp^{83}, and Asp^{84}) are close to oppositely charged residues of Bcl-x_L (Glu^{129}, Arg^{139}, and Arg^{100}, respectively) (Fig. 2).

Table 1. Binding affinities (*14*) of peptides to Bcl-x_L. Residues of Bak peptide substituted with alanine are in boldface. Abbreviations for the amino acid residues are as follows: A, Ala; C, Cys; D, Asp; E, Glu; F, Phe; G, Gly; H, His; I, Ile; K, Lys; L, Leu; M, Met; N, Asn; P, Pro; Q, Gln; R, Arg; S, Ser; T, Thr; V, Val; W, Trp; and Y, Tyr.

Peptide	Sequence		K_D (μM)
Bak	72 GQVGRQLAIIGDDINRRYDSEFQ	94	0.20 ± 0.02
	72 GQVGRQLAIIGDDINR.....	87	0.34 ± 0.03
	77 .....QLAIIGDDINR.....	87	No binding
	GQ**A**GRQLAIIGDDINR.....		15 ± 3
	GQVG**A**QLAIIGDDINR.....		3.3 ± 1
	GQVGRQ**A**AIIGDDINR.....		270 ± 90
	GQVGRQLA**A**IGDDINR.....		1.0 ± 0.2
	GQVGRQLAI**A**GDDINR.....		17 ± 6
	GQVGRQLAII**A**DDINR.....		0.50 ± 0.1
	GQVGRQLAIIG**A**DINR.....		41 ± 4
	GQVGRQLAIIGD**A**INR.....		0.14 ± 0.02
	GQVGRQLAIIGDD**A**NR.....		93 ± 20
Bcl-2	91 PVVHLALRQAGDDFSR.....	106	6.4 ± 0.8
Bax	57 KKLSECLKRIGDELDS.....	72	13 ± 3
Bik	55 DALALRLACIGDEMDV.....	70	15 ± 6
Bcl-x_L	84 AAVKQALREAGDEFEL.....	99	325

To identify the interactions that are important for complex formation, we measured the binding affinities of mutant Bak peptides containing alanine substitutions (Table 1) (*14*). A decrease in binding affinity by a factor of 800 was observed for the Bak peptide in which Leu^{78} is substituted by an alanine. This can be explained by the loss of extensive interactions between the side chain of Leu^{78} of Bak and the hydrophobic pocket formed by Tyr^{101}, Leu^{108}, Val^{126}, and Phe^{146} of Bcl-x_L (Fig. 2B). Mutation of other hydrophobic residues of Bak (Ile^{85}, Ile^{81}, and Val^{74}) to alanine also resulted in reduced binding to Bcl-x_L (Table 1), which further demonstrates the importance of hydrophobic interactions in complex formation. The hydrophobic residues at these positions are largely conserved in the Bcl-2 family of proteins (Table 1). In contrast, Ile^{80} is not conserved and is located on the surface of the complex (Fig. 2), consistent with the negligible loss in binding affinity observed when this residue was changed to an alanine.

Analysis of the structure (Fig. 2) suggested that the interaction between Asp^{83} of the Bak peptide and Arg^{139} of Bcl-x_L would stabilize complex formation. Indeed, Asp^{83} is completely conserved within the Bcl-2 family of proteins, and when substituted with alanine in the Bak peptide, markedly reduced the binding of this peptide to Bcl-x_L (Table 1). Moreover, Arg^{139} is highly conserved, and mutation of Arg^{139} to Gln in Bcl-x_L inhibits its antiapoptotic activity and binding to the Bax protein (*20*). It was also expected from the structure (Fig. 2) that electrostatic interactions between Arg^{76} of Bak and Glu^{129} of Bcl-x_L would contribute to complex formation. This is supported by the observed decrease in binding to Bcl-x_L of a Bak peptide in which Arg^{76} is mutated to alanine (Table 1).

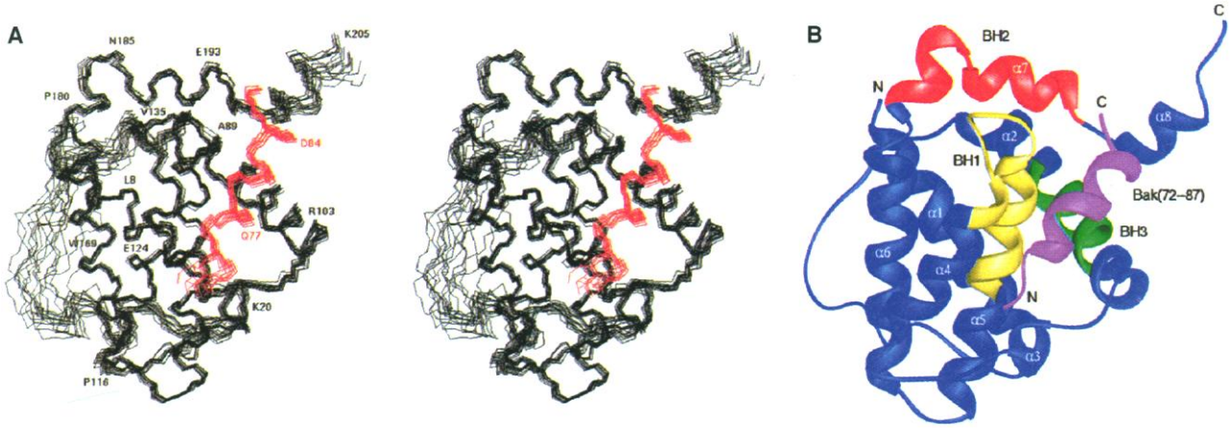

Fig. 1. (**A**) Stereoview of the backbone (N, C^{α}, C′) of 15 superimposed NMR-derived structures of Bcl-x_L (shown in black) complexed with the 16–amino acid Bak peptide (shown in red). (**B**) Ribbons (*21*) depiction of the averaged minimized NMR structure for the complex. The BH1, BH2, and BH3 regions of Bcl-x_L are shown in yellow, red, and green, respectively. The Bak peptide is shown in magenta.

However, the potential charge-charge interaction between Asp^{84} of Bak and Arg^{100} of Bcl-x_L does not appear to be critical for complex stabilization as a negligible effect on binding to Bcl-x_L was observed when Asp^{84} was substituted by an alanine (Table 1).

Interactions within the Bcl-2 family of proteins exhibit a defined selectivity and hierarchy (*12*, *13*). To investigate whether this selectivity is conferred by the BH3 regions from other Bcl-2 family members, we measured the binding affinities of a series of BH3-containing peptides to Bcl-x_L (*14*). Subtle differences in the amino acid sequences of the BH3 regions among members of the Bcl-2 family give rise to distinct differences in the affinities of these peptides for Bcl-x_L (Table 1). The Bak peptide binds to Bcl-x_L with greater affinity than any of the other peptides, including the peptides derived from the other death-promoting proteins, Bax and Bik. The Bcl-x_L peptide binds with the weakest affinity to Bcl-x_L, consistent with the monomeric nature of this protein (*11*). The selectivity of Bcl-x_L that we observed for the peptides from different Bcl-2 family members is consistent with the selectivity for heterodimer formation amongst the Bcl-2 family of proteins and suggests that the BH3 region plays a central role in defining the binding specificity of the Bcl-2–related proteins for Bcl-x_L.

The molecular interactions that stabilize the Bcl-x_L–Bak peptide complex likely reflect the important interactions that occur between the full-length proteins. The wild-type Bak peptide can inhibit the interaction of Bcl-x_L with full-length Bak or Bax in a concentration-dependent manner (*20*). Furthermore, Bak peptides containing alanine substitutions for Leu^{78} and Asp^{83}, which markedly reduced their binding to Bcl-x_L (Table 1), were unable to block heterodimer formation between-full length Bcl-x_L and Bak (Fig. 3A). When these two residues (Leu^{78} and Asp^{83}) were mutated in the full-length Bak protein, the mutant Bak proteins failed to coprecipitate with Bcl-x_L even though they were expressed at levels comparable to that of the wild type protein (Fig. 3B). Thus, the reduction in binding to Bcl-x_L observed with the full-length mutant Bak proteins resembles the loss in binding to Bcl-x_L measured for the mutant Bak peptides. These data are consistent with previous reports (*7*–*10*) on the functional importance of the BH3 region of the death-promoting proteins. This region of Bak and similar sequences in Bax and Bik (Bip1) promote apoptosis and interact with Bcl-x_L (*7*, *8*). In addition, neither the BH1 nor the BH2 region of Bax is necessary for binding to Bcl-2 or for promoting cell death (*9*, *10*).

Using the structure of the Bcl-x_L–Bak peptide complex and a homology model of the Bak protein, we modeled the structure of the heterodimer of the full-length proteins. In the structure of Bak based on its homology to Bcl-x_L, the hydrophobic side chains of the amphipathic α2 helix containing the BH3 region point toward the interior of the Bak protein, making these residues unavailable to interact with Bcl-x_L. Thus, binding to Bcl-x_L would necessitate a conformational change in the Bak protein to expose the hydrophobic surface of α2. One possibility is a rotation of the α2 helix along the helix axis that would allow the formation of the same hydrophobic and charge-charge interactions observed in the NMR structure of the Bcl-x_L–Bak peptide complex. It is of interest that based on the structure of Bcl-x_L, this helix is predicted to be flanked by highly flexible loops on both ends that could allow such a rotation.

In summary, our structure of the Bcl-x_L–Bak peptide complex reveals the structural basis for the requirements of the BH1, BH2, and BH3 regions for heterodimer formation among Bcl-2 family members. These data suggest that the formation of a hydrophobic binding cleft and properly positioned charged residues are required for the anti-apoptotic functions of Bcl-x_L. Indeed, a variety of mutations that would be predicted to alter the accessibility or binding properties of this region in Bcl-x_L and Bcl-2, including G138A (*3*), R139Q (*20*), Y101K (*20*), and L130A (*20*), have been shown to inhibit the function of this protein. For proteins that promote cell death, only the BH3 region is required for activity (*7*–*10*), which as shown here forms an amphipathic α helix and binds with high affinity to the hydrophobic groove in Bcl-x_L. Some proteins that promote cell death—such as Bik—have homology to other Bcl-2 pro-

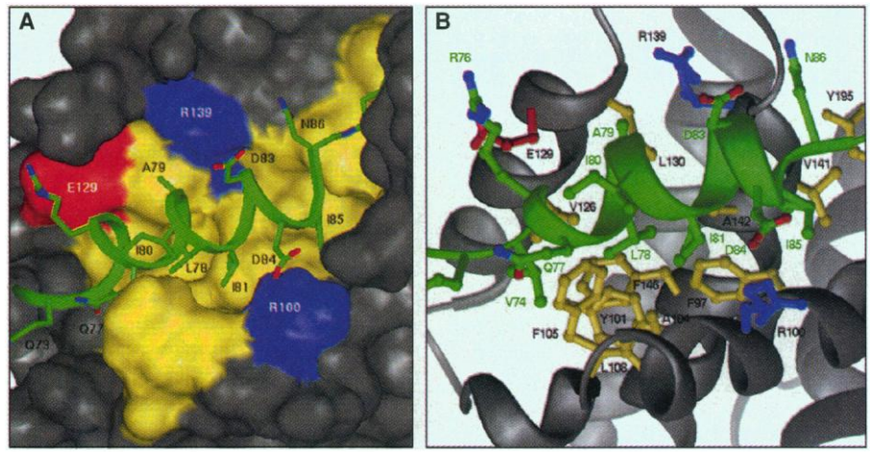

Fig. 2. (**A**) Surface representation of the binding pocket of Bcl-x_L bound to the Bak peptide. Hydrophobic residues showing NOEs to the peptide are colored in yellow, whereas Arg^{139}/Arg^{100} and Glu^{129} are colored in blue and red, respectively. Residues of Bcl-x_L are labeled in white and the Bak peptide in black. (**B**) Depiction of the side chains in the binding site of Bcl-x_L. Hydrophobic side chains of the protein showing NOEs to the peptide are colored in yellow. Side chains of positively and negatively charged side chains interacting with the peptide are colored in blue and red, respectively. The peptide side chains are colored by atom type. Residues of Bcl-x_L and the Bak peptide are labeled in black and green, respectively.

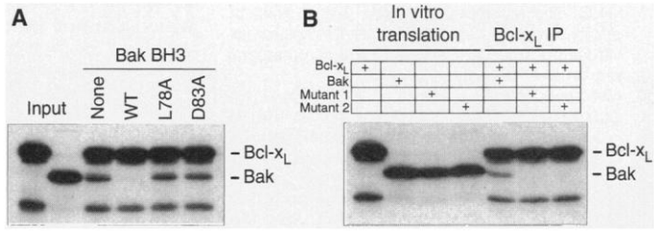

Fig. 3. (**A**) Mutations of critical residues in the Bak BH3 peptide abolish its ability to inhibit Bcl-x_L heterodimerization with Bak. In vitro–translated Bcl-x_L and Bak were combined together with 100 μM of the indicated Bak BH3 peptide. The reaction was immunoprecipitated with an antibody to Bcl-x (anti-Bcl-x), and the immunoprecipitated products were resolved by SDS–polyacrylamide gel electrophoresis (PAGE). (**B**) Mutations in Bak BH3 residues that are predicted to be involved in Bcl-x_L–Bak interactions abolish heterodimerization. In vitro–translated Bcl-x_L, Bak, or mutants of Bak were combined as indicated and immunoprecipitated with anti–Bcl-x. The immunoprecipitated products were resolved by SDS-PAGE. Bak mutation 1 contains a glutamic acid in place of arginine at amino acid 76 and an arginine in place of aspartic acid at amino acid 83. Bak mutant 2 contains an alanine in place of leucine at amino acid 78.

teins only within the BH3 region. In contrast, other Bcl-2–related proteins such as Bak or Bax are predicted to have more extensive structural similarities to Bcl-x_L. For these proteins, our studies suggest that a structural change may be required for the BH3 region to participate in dimerization.

REFERENCES AND NOTES

1. C. B. Thompson, *Science* **267**, 1456 (1995).
2. J. C. Reed, *J. Cell Biol.* **124**, 1 (1994).
3. X.-M. Yin, Z. N. Oltvai, S. J. Korsmeyer, *Nature* **369**, 321 (1994).
4. Z. N. Oltvai and S. J. Korsmeyer, *Cell* **79**, 189 (1994).
5. M. Hanada, C. Aimé-Sempé, T. Sato, J. C. Reed, *J. Biol. Chem.* **270**, 11962 (1995).
6. E. H.-Y. Cheng, B. Levine, L. H. Boise, C. B. Thompson, J. M. Hardwick, *Nature* **379**, 554 (1996).
7. T. Chittenden *et al.*, *EMBO J.* **14**, 5589 (1995).
8. J. M. Boyd *et al.*, *Oncogene* **11**, 1921 (1995).
9. H. Zha, C. Aimé-Sempé, T. Sato, J. C. Reed, *J. Biol. Chem.* **271**, 7440 (1996).
10. J. Hunter and T. G. Parslow, *ibid.*, p. 8521.
11. S. W. Muchmore *et al.*, *Nature* **381**, 335 (1996).
12. T. Sato *et al.*, *Proc. Natl. Acad. Sci. U.S.A.* **91**, 9238 (1994).
13. T. W. Sedlak, *ibid.* **92**, 7834 (1995).
14. The binding affinities of peptides to full-length Bcl-x_L were measured from the fluorescence emission of the Trp residues of Bcl-x_L as a function of increasing peptide concentration. The excitation and emission wavelengths were 290 and 340 nm, respectively.
15. Unlabeled peptide (GQVGRQLAIIGDDINR) and a peptide uniformly ^{15}N-,^{13}C-enriched for the Gly, Ala, Val, Leu, and Ile residues were purchased from PeptidoGenic Research (Livermore, CA) and purified by reversed-phase high-performance liquid chromatography on a C8 column. NMR samples (1 to 3 mM) of a 1:1 protein-peptide complex were prepared in a 10 mM sodium phosphate buffer (pH 6.5) in ^2H_2O or a 9:1 mixture of H_2O and ^2H_2O.
16. The deletion mutant of Bcl-x_L used in the NMR studies lacks the putative COOH-terminal transmembrane region and residues 45 to 84, which constitute a flexible loop previously shown to be dispensible for the antiapoptotic activity of Bcl-x_L (*11*). The deletion mutant of Bcl-x_L was constructed from the expression vector for Bcl-x_L (residues 1 to 209) (*11*) by a procedure similar to that of M. P. Weiner *et al.* [*Gene* **151**, 119 (1994)]. Residue numbers correspond to full-length Bcl-x_L. Thus, in the Δ(45–84)Bcl-x_L construct used in this study, residues 44 and 85 are sequential. The Δ(45–84)Bcl-x_L construct also has four additional NH_2-terminal residues (numbers −3 to 0) due to cloning artifacts. We prepared uniformly ^{15}N- and ^{15}N-,^{13}C-labeled proteins by growing the *Escherichia coli* strain HMS174(DE3) overexpressing Bcl-x_L on a minimal medium containing $^{15}NH_4Cl$ with or without [U-^{13}C]glucose. We prepared uniformly ^{15}N-,^{13}C-labeled and fractionally deuterated protein by growing the cells in 75% ^2H_2O. The recombinant protein was purified by affinity chromatography on a nickel-IDA column (Invitrogen) followed by ion-exchange chromatography on an S-Sepharose column.
17. NMR spectra were acquired at 30°C on a Bruker DMX500 or AMX600 NMR spectrometer. The ^1H, ^{13}C, and ^{15}N resonances of the backbone and side chains were obtained with a sample containing the (U-^{15}N-,^{13}C)-labeled and 75% deuterated protein as described [T. Yamazaki, W. Lee, S. H. Arrowsmith, D. R. Muhandiram, L. E. Kay, *J. Am. Chem. Soc.* **116**, 11655 (1994); G. M. Clore and A. M. Gronenborn, *Methods Enzymol.* **239**, 349 (1994)]. The methyl groups of Val and Leu residues were stereospecifically assigned [D. Neri, T. Szyperski, G. Otting, H. Senn, K. Wüthrich, *Biochemistry* **28**, 7510 (1989)]. Distance restraints were obtained from ^{15}N- or ^{13}C-resolved 3D NOE spectra, and φ dihedral angle restraints were measured from $^3J_{H^N,H^\alpha}$ coupling constants [H. Kuboniwa, S. Grzesiek, F. Delaglio, A. Bax *J. Biomol. NMR* **4**, 871 (1994)]. To assign the NMR resonances of the peptide and obtain intra- and intermolecular distance restraints, we acquired 2D and 3D ^{15}N-,^{13}C-filtered experiments on a sample with (U-^{15}N-,^{13}C)-labeled protein and unlabeled peptide. Additional distance restraints from ^{15}N- and ^{13}C-separated NOE experiments were obtained with a sample of unlabeled protein complexed to the Bak peptide uniformly ^{15}N- and ^{13}C- labeled for Gly, Ala, Val, Leu, and Ile. The structure calculations were based on a distance geometry and simulated annealing protocol [J. Kuszewski, M. Nilges, A. T. Brünger *J. Biomol. NMR* **2**, 33 (1992)] with the program X-PLOR [A. T. Brünger, *X-PLOR Version 3.1*, Yale University, New Haven, CT (1992)]. NOE-derived distance restraints with a square-well potential (F_{noe} = 50 kcal mol^{-1} Å^{-2}) were used after each was categorized as strong (1.8 to 3.0 Å), medium (1.8 to 4.0 Å), or weak (1.8 to 5.0 Å) on the basis of the NOE intensity. An additional 138 distance restraints were included for 69 hydrogen bonds identified from the slowly exchanging amides and given bounds of 1.8 to 2.3 Å (H-O) and 2.8 to 3.3 Å (N-O). No distance restraint was violated by more than 0.35 Å in any of the final structures. For the ensemble, the residual NOE rmsd was 0.009 ± 0.003 Å and the E_{noe} was 15 ± 3 kcal mol^{-1}. Torsional restraints were applied to 71 φ angles (including five for the peptide) with values of −60 ± 40° (F_{cdih} = 200 kcal mol^{-1} rad^{-2}) for $^3J(H^N,H^\alpha)$ for coupling constants <5.8 Hz in α-helical regions. No torsional angle restraint was violated by more than 5° in any of the final structures. For the ensemble, the residual torsional rmsd was 0.11 ± 0.06° and the E_{cdih} was 0.1 ± 0.0 kcal mol^{-1}. The covalent geometries were well satisified as indicated by a small total energy (137 ± 10 kcal mol^{-1}). Although the Lennard-Jones potential was not used during any refinement stage, the final structures exhibited good van der Waals geometries as illustrated by an E_{L-J} of −1104 ± 12 kcal mol^{-1}.
18. The rmsd between the NMR structures of free and complexed Bcl-x_L for the C^α atoms within the common regular elements of secondary structure is 1.7 Å. When complexed to the Bak peptide, residues 101 to 103 form an extension of the second α helix, the third helix in Bcl-x_L is reduced to a single helical turn, and residues 198 to 205 form an additional helix.
19. M. Eberstadt, M. Sattler, S. W. Fesik, unpublished data.
20. B. Chang, A. J. Minn, C. B. Thompson, unpublished data.
21. M. J. Carson, *J. Mol. Graph.* **5**, 103 (1987).

22. Supported in part by research grants POI AI35294 (C.B.T.) and R37 CA48023 (C.B.T.) from the National Institutes of Health. Coordinates for the averaged minimized NMR structure of the Bcl-x_L–Bak peptide complex have been deposited in the Brookhaven Protein Data Bank (accession number 1BXL).

15 July 1996; accepted 9 December 1996

A Protein-Counting Mechanism for Telomere Length Regulation in Yeast

Stéphane Marcand,* Eric Gilson, David Shore†

In the yeast *Saccharomyces cerevisiae*, telomere elongation is negatively regulated by the telomere repeat–binding protein Rap1p, such that a narrow length distribution of telomere repeat tracts is observed. This length regulation was shown to function independently of the orientation of the telomere repeats. The number of repeats at an individual telomere was reduced when hybrid proteins containing the Rap1p carboxyl terminus were targeted there by a heterologous DNA-binding domain. The extent of this telomere tract shortening was proportional to the number of targeted molecules, consistent with a feedback mechanism of telomere length regulation that can discriminate the precise number of Rap1p molecules bound to the chromosome end.

Telomeres, the ends of linear eukaryotic chromosomes, are essential structures formed by specific protein-DNA complexes that protect chromosomal termini from degradation and fusion (*1*). One of the essential functions of telomeres is to allow the complete replication of chromosome ends, which cannot be accomplished by known DNA polymerases (*2*). The progressive loss of DNA that would occur after each round of replication is balanced by a ribonucleoprotein terminal transferase enzyme called telomerase, which specifically extends the 3′ G-rich telomeric strand in an RNA-templated reaction (*3*). In most organisms, telomeric DNA consists of a tandem array of short repeats. In yeast, the telomeric DNA is organized in a nonnucleosomal structure based on an array of the telomere repeat–binding protein Rap1p (*4*, *5*).

In the human germline, cells express telomerase and maintain a constant average telomere length. This initial size appears to determine the replicative life-span of somatic cells, in which telomerase activity is usually undetectable and telomere repeats are progressively lost at each cell division (*6*). In unicellular organisms like *S. cerevisiae*, telomere length is kept within a narrow size distribution, specific for a given strain,

S. Marcand, Department of Microbiology, College of Physicians and Surgeons, Columbia University, New York, NY 10032, USA, and Laboratoire de Biologie Moléculaire et Cellulaire, Ecole Normale Supérieure de Lyon, 69364 Lyon Cédex 07, France.
E. Gilson, Laboratoire de Biologie Moléculaire et Cellulaire, Ecole Normale Supérieure de Lyon, UMR49 CNRS/ENSL, 69364 Lyon Cédex 07, France.
D. Shore, Department of Microbiology, College of Physicians and Surgeons, Columbia University, New York, NY 10032, USA, and Department of Molecular Biology, University of Geneva, CH-1211 Geneva 4, Switzerland.

*Present address: Ecole Normale Supérieure de Lyon, 69364 Lyon Cédex 07, France.
†To whom correspondence should be addressed (at University of Geneva). E-mail: David.Shore@molbio.unige.ch